NEW RESULTS FROM THE L3 COLLABORATION *

M. FABRE

on behalf of the L3 Collaboration

Paul Scherrer Institut CH-5232 Villigen, Switzerland

(Received April 2, 1997)

We report on the measurement of W-boson pair-production with the L3 detector at LEP at a centre-of-mass energy of 161.34 GeV and preliminary results at 172.13 GeV. In a data sample corresponding to a total luminosity of 11 pb^{-1} at 161.34 GeV and 10.25 pb^{-1} at 172.13 GeV, we select four-fermion events with high invariant masses of pairs of hadronic jets or leptons. Experimental results are given for the W-boson mass, cross sections and anomalous couplings.

PACS numbers: 12.15. -y, 14.70. Fm

1. Introduction

In the first half of the 1996 data taking period, the e^+e^- collider LEP at CERN was operated at a centre-of-mass energy, $\sqrt{s}$, of 161.34 GeV. This centre-of-mass energy coincides with the kinematic threshold of the process $e^+e^- \to W^+W^-$, thus allowing for the first time the pair-production of $W^\pm$ bosons in e^+e^- interactions. During this run the L3 detector collected a total integrated luminosity of 11 pb^{-1}. In the second half of the 1996 data taking period, L3 collected a total integrated luminosity of 10.25 pb^{-1} at a centre-of-mass energies, $\sqrt{s}$, of 172.32 GeV.

To lowest order, three Feynman diagrams contribute to W-pair production, the s-channel γ and Z-boson exchange and the t-channel ν_e exchange [1], referred to as CC03 [2, 3]. The W boson decays into a quark-antiquark pair, for example $W^- \to \bar{u}d$ *or* $\bar{c}s$, or a lepton-antilepton pair, $W^- \to \ell^-\bar{\nu}_\ell$, in the following denoted as qq and $\ell\nu$ for both W^+ and W^- decays. In this article, we report on measurements of all four-fermion final states mediated by W-pair production:

* Presented at the Cracow Epiphany Conference on W Boson, Cracow, Poland, January 4-6 1997.

1. $e^+e^- \to qq\epsilon\nu(\gamma)$ 2. $e^+e^- \to qq\mu\nu(\gamma)$ 3. $e^+e^- \to qq\tau\nu(\gamma)$
4. $e^+e^- \to l\nu l\nu(\gamma)$ 5. $e^+e^- \to qqqq(\gamma)$,

where (γ) indicates the possible presence of radiative photons.

Additional contributions to the production of these four-fermion final states arise from other neutral-current (NC) or charged-current (CC) Feynman diagrams. For high invariant masses of pairs of fermions and for the visible fermions all within the acceptance of the detector, the additional contributions are small. At the current level of statistical accuracy they need to be taken into account only for $e^+e^- \to qq\epsilon\nu(\gamma)$(CC20) and $e^+e^- \to l\nu l\nu(\gamma)$(CC56+NC56) [2, 3].

2. The L3 detector

The L3 detector [4] consists of a silicon micro-strip detector [5], a central tracking chamber, a high-resolution electromagnetic calorimeter composed of BGO crystals, a lead-scintillator ring calorimeter at low polar angles [6], a scintillation counter system, a uranium hadron calorimeter with proportional wire chamber readout, and an accurate muon chamber system. A forward-backward muon detection system extends the polar angle coverage of the muon chambers down to 24 degrees in the forward-backward region [7]. These detectors are installed in a 12 m diameter magnet which provides a solenoidal field of 0.5 T and a toroidal field of 1.2 T. The luminosity is measured using BGO calorimeters [8] situated on each side of the detector.

The response of the L3 detector is modelled with the GEANT [9] detector simulation program which includes the effects of energy loss, multiple scattering and showering in the detector materials and in the beam pipe.

3. Measurement of four-Fermion production

The analyses described below reconstruct the four-fermion final states. Charged leptons are explicitly identified using their characteristic signature. Hadronic jets are reconstructed by combining calorimetric energy depositions using the Durham jet algorithm [10]. Calorimetric clusters are treated as massless and are combined adding their four-momenta. The momentum of the neutrino in $qql\nu$ events is identified with the missing momentum vector.

Selection efficiencies and background contaminations of all processes are determined by Monte Carlo simulations. The following Monte Carlo event generators are used to simulate the various signal and background reactions:
KORALW [11] ($e^+e^- \to WW \to ffff(\gamma)$);
EXCALIBUR [12] ($e^+e^- \to ffff(\gamma)$);
PYTHIA [13]($e^+e^- \to q\bar{q}(\gamma), ZZ(\gamma)$, hadronic two-photon collisions);

KORALZ [14] ($e^+e^- \to \mu^+\mu^-(\gamma)$, $\tau^+\tau^-(\gamma)$);
BHAGENE3 [15]($e^+e^- \to e^+e^-(\gamma)$).

4. Event selection

The selections described bellow are a short illustrative summary, they do not contain all the selection criteria but only the most important ones. A complete description of the cuts, efficiencies and accepted background cross sections is given in [16]. The results on number of selected events, cross sections and couplings are determined in a combined fit as discussed in Section 5, results are summarised in Table I.

4.1. $e^+e^- \to qqe\nu(\gamma)$

The event selection for the process $e^+e^- \to qqe\nu(\gamma)$ requires an identified electron, missing momentum due to the neutrino, and high multiplicity arising from the qq system. A $qqe\nu$ event selected in the data is shown in Fig. 1.

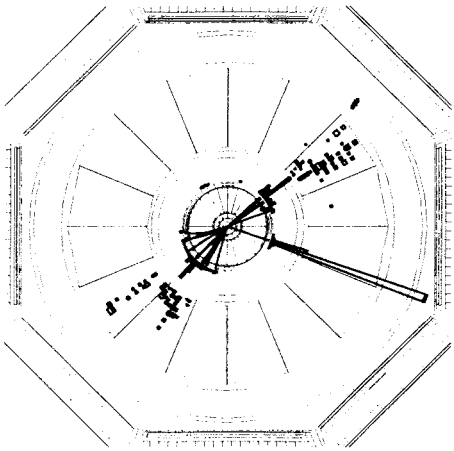

Fig. 1. A $qqe\nu$ event candidate. The kinematic quantities of this event are measured to be: $E_e = 36$ GeV, $E_\nu = 45$ GeV, $M_{qq} = 90$ GeV and $M_{e\nu} = 80$ GeV.

The electron is identified in the electromagnetic calorimeter as the highest energy deposition with electromagnetic shower shape. This calorimetric cluster must have a polar angle of $|\cos\theta_e| < 0.90$ and an energy E_e larger than 25 GeV. The neutrino energy E_ν, inferred from the missing momentum of the event, must be larger than 25 GeV. In order to reject radiative $q\bar{q}(\gamma)$ events where the photon escapes along the beam pipe, the polar an-

gle of the missing momentum vector must point well inside the detector, $|\cos\theta_\nu| < 0.90$. After having removed the calorimetric energy depositions associated with the identified electron, the remaining calorimetric clusters are grouped into two jets. The masses of the two W bosons are calculated as the invariant masses of the electron-neutrino system, $M_{e\nu}$, and the jet-jet system, M_{qq}. Both invariant masses are required to be larger than 50 GeV.

The signal efficiency is determined within the following generator level cuts: $E_e, E_\nu > 25$ GeV; $|\cos\theta_e|, |\cos\theta_\nu| < 0.90$; $M_{e\nu}, M_{qq} > 50$ GeV.

4.2. $e^+e^- \to qq\mu\nu(\gamma)$

The event selection for the process $e^+e^- \to qq\mu\nu(\gamma)$ requires an identified muon, missing momentum due to the neutrino, and high multiplicity arising from the qq system. The muon is identified in the muon spectrometer as the highest momentum track pointing back to the interaction vertex. It must have a momentum larger than 20 GeV. Muons arising from decays of hadron are rejected by requesting the muon to be isolated and no secondary muon with more than 20 GeV momentum must be present. The calorimetric clusters are grouped into two jets. The masses of the two W bosons are calculated as the invariant masses of the muon-neutrino system and the jet-jet system. The muon-neutrino invariant mass must be larger than 55 GeV, and the jet-jet invariant mass must be larger than 40 GeV and smaller than 120 GeV.

4.3. $e^+e^- \to qq\tau\nu(\gamma)$

The event selection for the process $e^+e^- \to qq\tau\nu(\gamma)$ is based on the identification of a tau jet in a hadronic event, combined with missing energy. The tau jet is identified as a low-energy electron or muon, or a low-multiplicity narrow jet, isolated from the rest of the event.

The tau lepton is identified by its decay products. Electrons and muons are identified according to the lepton identification described in the muon and electron selections. If the lepton energy is larger than 5 GeV and the sum of the lepton energy and the missing momentum less than 65 GeV, the identified electron or muon is considered as the tau jet.

If no electrons or muons are found, geometrical jets are reconstructed based on clustering inside a cone of 15 degrees half-opening angle. At least three jets with an energy larger than 10 GeV are required. Out of the three most energetic jets the two most back-to-back jets are associated with the qq system. The most energetic remaining jet is taken as the tau jet. The efficiency of this tau jet identification for hadronic tau decays is 83%.

The tau jet must contain one, two or three tracks reconstructed in the central tracking chamber. After having removed the tracks and calorimetric energy depositions associated with the identified tau jet, the remaining tracks and calorimetric clusters are grouped into two hadronic jets using the Durham jet algorithm. The tau jet must be separated by at least 25 degrees from the two hadronic jets. The invariant mass of the system of the two hadronic jets must be larger than 60 GeV and smaller than 100 GeV. The invariant mass of the system of the tau jet and the missing four-momentum must be larger than 55 GeV.

4.4. $e^+e^- \to l\nu l\nu(\gamma)$

The event selection for the process $e^+e^- \to l\nu l\nu(\gamma)$ requires two leptons and missing energy due to the neutrinos. Low-multiplicity leptonic final states are selected by requiring between one and six tracks in the central tracking chamber and less than 15 calorimetric clusters. The visible energy of the event is required to be larger than 2% and smaller than 80% of $\sqrt{s}$.

Final states from hadronic tau decays are identified as geometrical jets which are reconstructed based on a clustering inside a cone of 30 degrees half-opening angle. At least one identified electron or muon with an energy between 20 GeV and 70 GeV is required.

In the lepton-lepton class, the acoplanarity between the two leptons is required to be larger than eight degrees in order to reject $l^+l^-(\gamma)$ events. In the lepton-jet class, a jet with more than 8 GeV energy is required. In order to reject $l^+l^-(\gamma)$ events the acoplanarity between the lepton and the jet as well as between the lepton and any track in the central tracking chamber must be larger than eight degrees.

The signal efficiency is determined within the following generator level cuts: $|\cos\theta| < 0.96$ for both charged leptons, with energies larger than 15 GeV and 5 GeV.

4.5. $e^+e^- \to qqqq(\gamma)$

The event selection for the process $e^+e^- \to qqqq(\gamma)$ requires a four-jet signature, with kinematics compatible with a WW intermediate state. The main background arises from the process $e^+e^- \to q\bar{q}(\gamma)$, which can lead to multi-jet final states through gluon radiation and jet reconstruction and has a total cross section about two orders of magnitude larger than the expected signal.

A preselection is applied which accepts 88.4% of the $WW \to qqqq(\gamma)$ signal while reducing the dominating $q\bar{q}(\gamma)$ background by a factor of 21. Two pairs of jets are formed, corresponding to the two W bosons. The chosen

jet-jet pairing maximises the sum of the two jet-jet invariant masses, which yields the correct assignment for about 80% of the selected $WW \to qqqq(\gamma)$ events.

Because of the very high $q\bar{q}(\gamma)$ background and the similar topology of four-jet events arising in WW and $q\bar{q}$ production, a neural network is used to improve their separation. A three-layer feed-forward neural network with twelve input nodes, one hidden layer with 15 nodes, and one output node is trained on signal and background Monte Carlo such that the output peaks at 1 for the signal, and at 0 for the background. The twelve input variables consist of event shape variables sensitive to the general four-jet topology, to the signal kinematics and to the background topology.

The output of the neural network for data events is fitted by a linear combination of neural-network output distributions derived from Monte Carlo simulations for signal and background. The distribution of the neural-network output is shown in Fig. 2. A maximum-likelihood fit is used to determine the fraction of $qqqq(\gamma)$ signal events in the total sample of selected events.

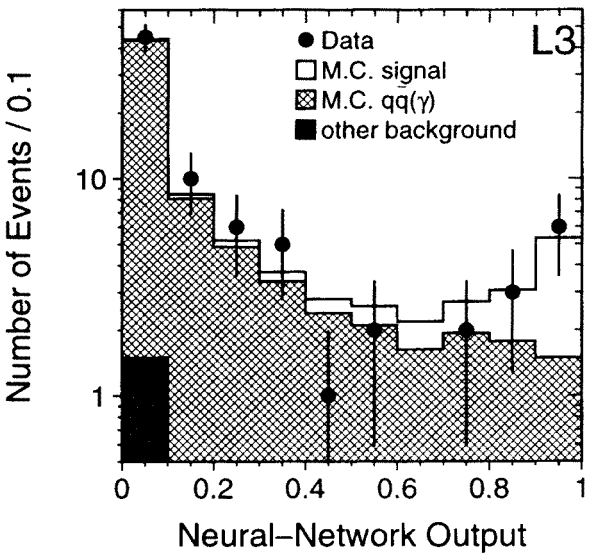

Fig. 2. Distribution of the output of the neural network used in the analysis of $e^+e^- \to qqqq(\gamma)$ events, comparing the data to the signal and background Monte Carlo. All selection cuts are applied.

5. Results at $\sqrt{s} = 161.3$ GeV

Cross sections

The cross sections, σ_i, of the signal processes i are determined simultaneously in one maximum-likelihood fit. The total likelihood is given by the product of Poissonian probabilities, $P(N_i, \mu_i)$, corresponding to the signal processes i having N_i selected events (Table I). The expected number of events for process i, μ_i, is calculated as:

$$\mu_i = \left(\sum_{j=1}^{5} \varepsilon_{ij} \sigma_j + \sigma_i^{\mathrm{bg}} \right) \cdot \mathcal{L}_i \ , \tag{5.1}$$

where ε_{ij} is the efficiency of selection i to accept events from process j, σ_i^{bg} is the remaining background cross section arising from other processes, and $\mathcal{L}_i$ is the luminosity used in the analysis. For the $\mathrm{e^+e^-} \to qqqq(\gamma)$ process, the Poissonian probability is replaced by the likelihood as a function of the signal cross section derived from the fit described in Section 4.5. Statistical errors corresponding to a 68% confidence level interval are determined by a change of 0.5 in the logarithm of the total likelihood. The resulting cross sections and their statistical errors as given by the fit are listed in Table I.

For the $qq\mathrm{e}\nu(\gamma)$ and $l\nu l\nu(\gamma)$ final state the measured cross sections contain significant contributions from processes not mediated by resonant W-pair production. In order to determine W-pair cross sections also for these final states the measured cross sections are scaled by a multiplicative factor, f_i. These conversion factors are given by the ratio of the total CC03 cross section and the four-fermion cross section within cuts, and are calculated within the Standard Model using the EXCALIBUR [12] event generator. They are determined to be 1.27 for $qq\mathrm{e}\nu(\gamma)$ and 0.92 for $l\nu l\nu(\gamma)$, where the dependence of f_i on M_W is negligible. These cross sections for the $qq\mathrm{e}\nu(\gamma)$ and $l\nu l\nu(\gamma)$ final states are also listed in Table I.

W-pair cross section and W-decay branching fractions

For the determination of the total CC03 production cross section of W-pairs, σ_{WW}, the ansatz described above is modified. The channel cross sections σ_i are replaced by the product $r_i\sigma_{\mathrm{WW}}$ or $r_i\sigma_{\mathrm{WW}}/f_i$ for the $qq\mathrm{e}\nu(\gamma)$ and $l\nu l\nu(\gamma)$ final states. The ratio r_i is the ratio between the CC03 cross section for process i and σ_{WW}. They are given in terms of the W-decay branching fractions, $B(W \to qq)$ and $B(W \to l\nu)$, as follows: $r_{qqqq} = [B(W \to qq)]^2$, $r_{qql\nu} = 2B(W \to qq)B(W \to l\nu)$, and $r_{l\nu l\nu} = [1 - B(W \to qq)]^2$, where the sum of the hadronic and the three leptonic branching fractions is constrained to be unity.

TABLE I

Total luminosity used in the analyses, $\mathcal{L}$, number of selected data events, N_{data}, number of expected non-W background events, N_{bg}, and CC03 cross sections. For the processes $e^+e^- \to qqe\nu(\gamma)$ and $e^+e^- \to l\nu l\nu(\gamma)$ the cross section within generator level cuts is also given. The errors are statistical only.

Process	$\mathcal{L}$ [pb^{-1}]	N_{data}	N_{bg}	σ(cuts) [pb]	σ(CC03) [pb]
$e^+e^- \to qqe\nu(\gamma)$	10.2	4	0.16	$0.49^{+0.30}_{-0.22}$	$0.62^{+0.38}_{-0.27}$
$e^+e^- \to qq\mu\nu(\gamma)$	10.9	4	0.18	—	$0.53^{+0.33}_{-0.24}$
$e^+e^- \to qq\tau\nu(\gamma)$	10.2	3	1.61	—	$0.22^{+0.55}_{-0.38}$
$e^+e^- \to l\nu l\nu(\gamma)$	9.6	2	0.39	$0.42^{+0.46}_{-0.29}$	$0.39^{+0.43}_{-0.27}$
$e^+e^- \to qqqq(\gamma)$	10.2	8.9	—	—	$0.98^{+0.51}_{-0.40}$

TABLE II

W-decay branching fractions, B, and total W-pair cross section, σ_{WW}, derived with and without the assumption of charged-current lepton universality.

Parameter	Lepton Non-Universality	Lepton Universality
$B(W \to e\nu)$ [%]	18^{+11}_{-8}	—
$B(W \to \mu\nu)$ [%]	16^{+10}_{-7}	—
$B(W \to \tau\nu)$ [%]	6^{+12}_{-11}	—
$B(W \to l\nu)$ [%]	—	$13^{+\ 3}_{-\ 3}$
$B(W \to qq)$ [%]	61^{+10}_{-11}	$60^{+\ 9}_{-10}$
σ_{WW} [pb]	$2.73^{+0.87}_{-0.74}$	$2.94^{+0.84}_{-0.72}$
Parameter	Using SM W-Decay Branching Fractions	
σ_{WW} [pb]	$2.89^{+0.81}_{-0.70}$	

The total W-pair cross section and the W-decay branching fractions as determined from fits to the data are listed in Table II. They are determined both with and without the assumption of charged-current lepton universality in W decays. The W-decay branching fractions obtained for the individual leptons are in agreement with each other. This is the first direct determination of the branching fraction of the W to hadrons. In order to obtain an improved determination of σ_{WW}, the W-decay branching fractions from the Standard Model are imposed, which are calculated including QCD and mass corrections [3] (Table II). The result for the total production cross section of W-pairs at $\sqrt{s} = 161.34 \pm 0.06$ GeV [17] is:

$$\sigma_{\mathrm{WW}} = 2.89^{+0.81}_{-0.70}\ (\mathrm{stat.}) \pm 0.14\ (\mathrm{syst.})\ \mathrm{pb}\ , \tag{5.2}$$

where the first error is statistical and the second systematic. This value for σ_{WW} agrees well with other recent measurements of σ_{WW} at $\sqrt{s} = 161$ GeV [18, 19].

W mass

Within the Standard Model the measured cross sections, σ_i, depend on $\sqrt{s}$ and the mass of the W boson, M_W. In order to determine a value for M_W, the cross-section fit to the data is repeated with the cross sections σ_i of Eq. (5.1) replaced by the functions $\sigma_i(\sqrt{s}, M_W)$, leaving M_W as the only free parameter. Using the Standard-Model calculations of $\sigma_i(\sqrt{s}, M_W)$ as implemented in GENTLE [20] (CC03) and EXCALIBUR [12] ($qq e\nu(\gamma)$ and $l\nu l\nu(\gamma)$ final states), M_W is found to be:

$$M_W = 80.80^{+0.48}_{-0.42}\ (\mathrm{exp.}) \pm 0.03\ (\mathrm{LEP})\ \mathrm{GeV}.$$

The same result for M_W is obtained using only the total W-pair cross section of Equation (5.2), as shown in Fig. 3. The second error on M_W arises from the uncertainty in the calibration of the LEP beam energy [17].

This value for M_W agrees well with our indirect determination of M_W from measurements at the Z resonance [21], and with recent measurements of M_W at $\mathrm{p\bar{p}}$ colliders [22, 23] and at LEP [18, 19].

6. Preliminary results at $\sqrt{s} = 172$ GeV

In the second half of the 1996 data taking period, the $\mathrm{e^+e^-}$ collider LEP at CERN was operated at centre-of-mass energies, $\sqrt{s}$, of 172.32 GeV [17]. The higher centre-of-mass energy implies an increased cross section for the W-pair signal and a reduced cross section for the background, improving the signal-to-background ratio by a factor of about four.

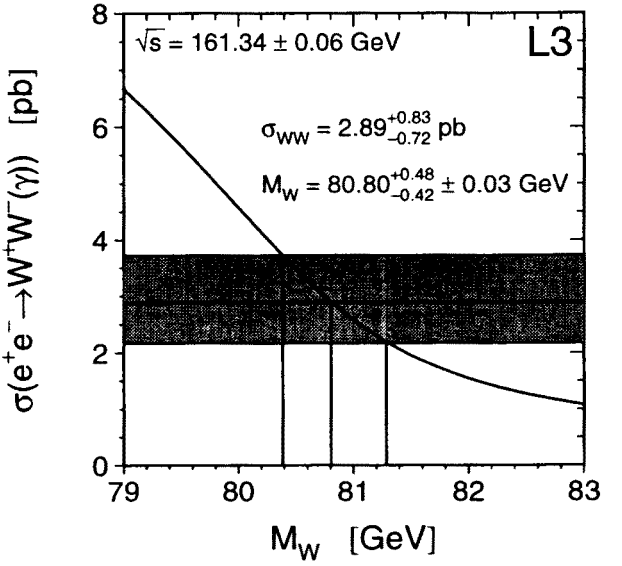

Fig. 3. The cross section, σ_{WW}, of the process $e^+e^- \to WW \to ffff(\gamma)$ as a function of the W-mass, M_W. The horizontal band shows the cross-section measurement with its total error, combining statistical and systematic error in quadrature. The curve shows the Standard Model expectation and is computed with the GENTLE [20] program. The second error on M_W arises from the LEP beam energy calibration [17].

Cross sections and W-decay branching fractions

Most event selections are similar to those at 161 GeV, adapted to the higher centre-of-mass energy. An exception is the $qqqq$ selection which is not using a neural network. The fit method used to extract the cross sections is identical to the one described above. The results of this fit are listed in Table III.

TABLE III

Total luminosity used in the analyses, $\mathcal{L}$, number of selected data events, $N_{\rm data}$, number of expected non-W background events, $N_{\rm bg}$, and CC03 cross sections. For the processes $e^+e^- \to qqe\nu(\gamma)$ and $e^+e^- \to l\nu l\nu(\gamma)$ the cross section within generator level cuts is also given. The errors are statistical only.

Process	$\mathcal{L}$ [pb^{-1}]	$N_{\rm data}$	$N_{\rm bg}$	σ(cuts) [pb]	σ(CC03) [pb]
$e^+e^- \to qqqq(\gamma)$	10.25	59	15.7	—	$5.51^{+1.03}_{-0.94} \pm 0.28$
$e^+e^- \to qqe\nu(\gamma)$	10.25	19	0.75	$2.16^{+0.57}_{-0.49} \pm 0.15$	$2.37^{+0.63}_{-0.54} \pm 0.17$
$e^+e^- \to qq\mu\nu(\gamma)$	10.25	10	0.36	—	$1.14^{+0.44}_{-0.35} \pm 0.06$
$e^+e^- \to qq\tau\nu(\gamma)$	10.25	15	2.60	—	$2.14^{+0.91}_{-0.77} \pm 0.13$
$e^+e^- \to l\nu l\nu(\gamma)$	9.76	10	0.19	$2.24^{+0.80}_{-0.65} \pm 0.07$	$2.30^{+0.82}_{-0.67} \pm 0.07$

The data collected at 161 GeV and at 172 GeV are combined for the determination of the W-decay branching fractions. The W-decay branching fractions obtained for the individual leptonic decay modes are in agreement with each other. Assuming charged-current lepton universality, the branching fraction for the decay of the W boson to hadrons is found to be:

$$B(W \to \text{hadrons}) = 62.3^{+3.9}_{-4.0}\ (\text{stat.}) \pm 0.8\ (\text{syst.})\ \%, \qquad (6.1)$$

the branching fraction for the decay of the W boson to leptons is found to be:

$$B(W \to l\nu) = 12.6^{+1.3}_{-1.3}\ (\text{stat.}) \pm 0.3\ (\text{syst.})\ \%, \qquad (6.2)$$

in good agreement with the Standard-Model expectation of 67.5 % and 10.8 % respectively. Assuming Standard-Model W-decay branching fractions, the total W-pair cross section at $\sqrt{s} = 172.13$ GeV [17] is measured to be:

$$\sigma_{\rm WW} = 12.93^{+1.50}_{-1.41}\ (\text{stat.}) \pm 0.38\ (\text{syst.})\ \text{pb}. \qquad (6.3)$$

The cross sections for W-pair production measured at 161 GeV and at 172 GeV are compared to the Standard-Model expectations in Fig. 4. Good agreement is observed.

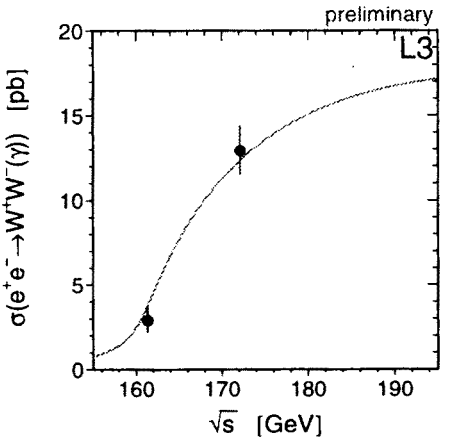

Fig. 4. The W-pair cross section as a function of centre-of-mass energy. The curve shows the Standard Model expectation for a W mass of $M_W = 80.356$ GeV [23].

Mass of the W boson

Based on the events as selected above, the mass of the W boson, M_W, is determined using the method of direct reconstruction [3]. Two W bosons are reconstructed in each event by grouping the four reconstructed final-state fermions in pairs. A kinematic fit imposing four-momentum conservation is applied to improve the determination of invariant masses.

Various methods to extract a value for the W boson mass, M_W, from the distribution of the reconstructed average invariant masses, M_{inv}, are studied, in particular the methods referred to as Monte Carlo calibration method, convolution method, and reweighting method in Section 3.3 of [3]. The results are in good agreement between all methods. In the following the results of unbinned maximum-likelihood fits to the data using the box method are quoted. The box method is a reweighting method where event weights are calculated summing over Monte Carlo events in small bins ("boxes") of reconstructed invariant mass centred around each data event.

The mass of the W boson is determined separately for the $qqqq$, $qqe\nu$ and $qq\mu\nu$ event samples, with the result:

$$
\begin{aligned}
M_W(qqqq) &= 80.79 \pm 0.50\ (\text{stat.}) \pm 0.07\ (\text{syst.}) \pm 0.10\ (th.) \pm 0.03\ (\text{LEP})\ \text{GeV}, \\
M_W(qqe\nu) &= 80.88 \pm 0.54\ (\text{stat.}) \pm 0.07\ (\text{syst.}) \pm 0.10\ (th.) \pm 0.03\ (\text{LEP})\ \text{GeV}, \\
M_W(qq\mu\nu) &= 80.12 \pm 0.86\ (\text{stat.}) \pm 0.07\ (\text{syst.}) \pm 0.02\ (th.) \pm 0.03\ (\text{LEP})\ \text{GeV}.
\end{aligned}
$$

The first error is the *expected* statistical error for an event sample of the size selected in the data. It is determined from the spread of the fitted central values for M_W obtained by fitting several Monte Carlo samples the size of the data samples. The second error is the experimental systematic error derived from comparing different event reconstruction and fitting methods. The third error is a theoretical error concerning the functional form of the invariant-mass spectrum. Especially, it contains a contribution of 100 MeV for the $qqqq$ final state arising from colour-reconnection and Bose-Einstein effects [3], and of 100 MeV for the $qq e\nu$ final state due to single- and non-resonant contributions. The last error arises from the calibration of the LEP beam energy [17].

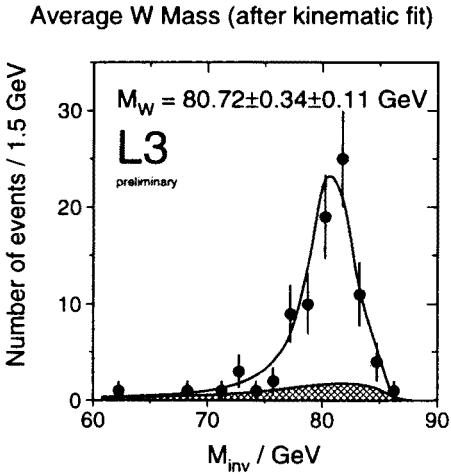

Fig. 5. The distribution of the reconstructed invariant masses, $M_{\rm inv}$, for $qqqq$, $qq e\nu$ and $qq\mu\nu$ events. The curve is the result of the fit. The hatched region shows the combined background which is dominated by $q\bar{q}(\gamma)$ events accepted by the $qqqq$ selection.

The results obtained for the different final states are in good agreement with each other. They are combined taking correlated systematic errors into account. The result on M_W thus obtained from the 172 GeV data is:

$$M_W = 80.72 \pm 0.34 \text{ (stat.)} \pm 0.11 \text{ (syst.)} \pm 0.03 \text{ (LEP) GeV}, \qquad (6.4)$$

as shown in Fig. 5. This result is in good agreement with our published result on M_W determined from the cross section at threshold (161 GeV), $M_W = 80.80^{+0.48}_{-0.42} \pm 0.03$ (LEP)GeV. Combining these results, the mass of the W boson is determined to be:

$$M_W = 80.75 \pm 0.28 \text{ (exp.)} \pm 0.03 \text{ (LEP) GeV}. \qquad (6.5)$$

Triple-vector-boson couplings

Alternatively, when the W mass is known, the total cross section can be interpreted in terms of triple-vector-boson couplings [24, 3]. In particular, it is interesting to test if the coupling between the Z and a pair of W bosons exists [25].

For the results presented in the following, the differential cross section in the W^- polar angle for selected $qqe\nu$ and $qq\mu\nu$ events is used together with the total cross section measured at 161 GeV and at 172 GeV.

The deviation, δ_Z, of the ZWW coupling, g_{ZWW}, from its Standard Model value of $\cot\theta_W = 1.9$ is found to be:

$$\delta_Z = g_{ZWW} - \cot\theta_W \tag{6.6}$$

$$= 0.0^{+1.1}_{-0.9} \ (68\%\ \mathrm{CL}) \tag{6.7}$$

$$= 0.0^{+2.0}_{-1.6} \ (95\%\ \mathrm{CL})\,. \tag{6.8}$$

This confirms the existence of the ZWW coupling at more than 95% CL. In an alternative scenario [3], where more than one anomalous coupling is introduced, but depending on a single parameter, $\alpha_{W\Phi}$, one finds:

$$\alpha_{W\Phi} = 0.0^{+0.4}_{-0.4} \ (68\%\ \mathrm{CL}) \tag{6.9}$$

$$= 0.0^{+0.7}_{-0.6} \ (95\%\ \mathrm{CL})\,. \tag{6.10}$$

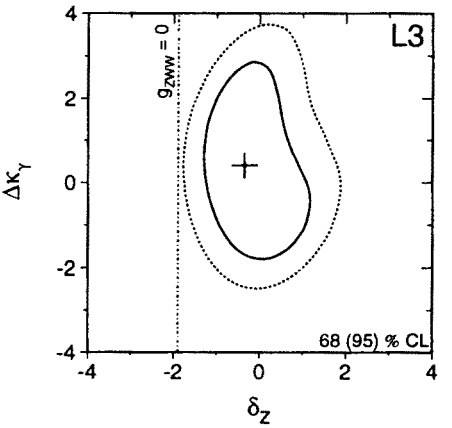

Fig. 6. Contour curves of 68% and 95% confidence level for the two anomalous triple-vector-boson couplings $\Delta\kappa_\gamma$ and δ_Z.

With the increased statistics at 172 GeV it is also possible to determine two triple-vector-boson couplings simultaneously, for example, an anomalous contribution to the magnetic dipole-moment of the W boson, $\Delta\kappa_\gamma = \kappa_\gamma - 1$, in addition to δ_Z. The result of a two-parameter fit to the data is:

$$\delta_Z = -0.4^{+1.1}_{-0.7} \ (68\% \text{ CL}), \tag{6.11}$$

$$\Delta\kappa_\gamma = +0.4^{+1.9}_{-1.8} \ (68\% \text{ CL}), \tag{6.12}$$

as shown in Fig. 6. The constraint $\Delta\kappa_\gamma = -\cot^2\theta_W(\Delta\kappa_Z - \delta_Z \tan\theta_W)$ [3] is imposed. In all scenarios good agreement with the Standard Model expectation of $\delta_Z = \alpha_{W\Phi} = \Delta\kappa_\gamma = 0$ is observed.

REFERENCES

[1] S.L. Glashow, *Nucl. Phys.***22**, 579 (1961); S. Weinberg, *Phys. Rev. Lett.***19**, 1264 (1967); A. Salam, *Elementary Particle Theory*, ed. N. Svartholm, Stockholm, Almquist and Wiksell (1968), p. 367.

[2] D. Bardin *et al.*, *Nucl. Phys.*(Proc. Suppl.) **B37**, 148 (1994); F.A. Berends *et al.*, *Nucl. Phys.*(Proc. Suppl.) **B37**, 163 (1994).

[3] Physics at LEP 2, Report CERN 96-01 (1996), eds G.Altarelli, T. Sjöstrand, F. Zwirner, Vol. 1 and Vol. 2.

[4] The L3 Collaboration, B. Adeva *et al.*, *Nucl. Instrum. Methods* **A289**, 35 (1990).

[5] M. Acciarri *et al.*, *Nucl. Instrum. Methods* **A351**, 300 (1994).

[6] M. Chemarin *et al.*, *Nucl. Instrum. Methods* **A349**, 345 (1994).

[7] A. Adam *et al.*, The Forward Muon Detector of L3, CERN-PPE/96-097.

[8] I.C. Brock *et al.*, *Nucl. Instrum. Methods* **A381**, 236 (1996).

[9] The L3 detector simulation is based on GEANT Version 3.15. R. Brun *et al.*, *GEANT 3*, CERN-DD/EE/84-1 (Revised), 1987. The GHEISHA program (H. Fesefeldt, RWTH Aachen Report PITHA 85/02 (1985)) is used to simulate hadronic interactions.

[10] S. Catani *et al.*, *Phys. Lett.* **B269**, 432 (1991).

[11] The KORALW version 1.21 is used. M. Skrzypek, S. Jadach, W. Płaczek, Z. Wąs, *Comput. Phys. Commun.* **94**, 216 (1996); M. Skrzypek, S. Jadach, M. Martinez, W. Płaczek, Z. Wş, *Phys. Lett.* **B372**, 289 (1996).

[12] F.A. Berends, R. Kleiss, R. Pittau, *Nucl. Phys.* **B424**, 308 (1994); *Nucl. Phys.* **B426**, 344 (1994); *Nucl. Phys.* (Proc. Suppl.) **B37**, 163 (1994); *Phys. Lett.* **B335**, 490 (1994); R. Kleiss, R. Pittau, *Comput. Phys. Commun.* **83**, 141 (1994).

[13] T. Sjöstrand, PYTHIA 5.7 and JETSET 7.4 Physics and Manual, CERN-TH/7112/93 (1993), revised August 1995; T. Sjöstrand, *Comput. Phys. Commun.***82**, 74 (1994).

[14] The KORALZ version 4.01 is used. S. Jadach, B.F.L. Ward, Z. Wąs, *Comput. Phys. Commun.***79**, 503 (1994).

[15] J.H. Field, *Phys. Lett.***B323**, 432 (1994); J.H. Field, T. Riemann, *Comput. Phys. Commun.***94**, 53 (1996).

[16] The L3 Collaboration, M. Acciari *et al.*, CERN-PPE/97-14 (1997).

[17] The working group on LEP energy, CERN-SL note, in preparation.

[18] The OPAL Collaboration, K. Ackerstaff *et al.*, Phys. Lett. **B389**, 416 (1996).

[19] The DELPHI Collaboration, P. Abreu *et al.*, Measurement and interpretation of the W-pair cross-section in e^+e^- interactions at 161 GeV, CERN-PPE/97-09.

[20] The GENTLE version 2.0 is used. D. Bardin *et al.*, GENTLE/4fan v. 2.0: A Program for the Semi-Analytic Calculation of Predictions for the Process $e^+e^- \to 4f$, DESY 96-233, hep-ph/9612409.

[21] The L3 Collaboration, M. Acciarri *et al.*, *Z. Phys.* **C62**, 551 (1994).

[22] The UA1 Collaboration, C. Albajar *et al.*, *Phys. Lett.* **B253**, 503 (1991); The UA2 Collaboration, J. Alitti *et al.*, *Phys. Lett.* **B276**, 365 (1992); The CDF Collaboration, F. Abe *et al.*, *Phys. Rev. Lett.* **74**, 341 (1995); *Phys. Rev.* **D52**, 2624 (1995); The DØ Collaboration, S. Abachi *et al.*, *Phys. Rev. Lett.* **75**, 1456 (1995). We use the average value and error for the total width of the W boson as listed in: R.M. Barnett *et al.*, *Phys. Rev.* **D54**, 1 (1996).

[23] M. Rijssenbeek, Measurements of the Mass of the W Boson from CDF/DØ, to appear in the proceedings of the 28th International Conference on High Energy Physics, 25-31 July 1996, Warsaw, Poland.

[24] K. Hagiwara *et al.*, *Nucl. Phys.* **B282**, 253 (1987).

[25] I. Kuss, D. Schildknecht, *Phys. Lett.* **B383**, 470 (1996).